



# Nitrogen deposition sources and patterns in the Greater Yellowstone Ecosystem determined from ion exchange resin collectors, lichens, and isotopes

Abigail S. Hoffman<sup>a,\*</sup>, Shannon E. Albeke<sup>a</sup>, Jill A. McMurray<sup>b</sup>, R. David Evans<sup>c</sup>, David G. Williams<sup>a</sup>

<sup>a</sup> University of Wyoming, Laramie, WY 82071, United States of America

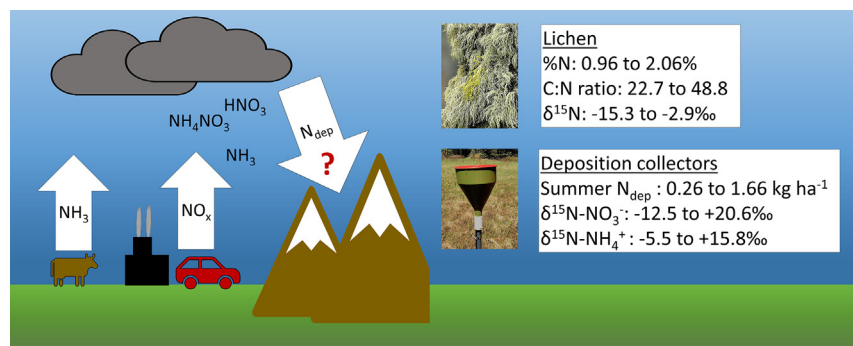
<sup>b</sup> Bridger Teton National Forest, United States Forest Service, Pinedale, WY 82941, United States of America

<sup>c</sup> School of Biological Sciences, Washington State University, Pullman, WA 99164, United States of America

## HIGHLIGHTS

- Patterns of  $N_{\text{dep}}$  were determined across the Greater Yellowstone Ecosystem.
- $\text{NO}_3^-$ ,  $\text{NH}_4^+$  and  $\delta^{15}\text{N}$  in resin collectors and  $\%N$  and  $\delta^{15}\text{N}$  from lichens were measured.
- $N_{\text{dep}}$  measured was high but variable for a remote, protected area.
- $\delta^{15}\text{N}$  suggested agricultural  $\text{NH}_x$  was a major source.
- C:N ratio has potential as a marker for ecological health.

## GRAPHICAL ABSTRACT



## ARTICLE INFO

### Article history:

Received 30 December 2018

Received in revised form 20 May 2019

Accepted 21 May 2019

Available online 22 May 2019

### Keywords:

Throughfall N deposition

$\delta^{15}\text{N}$

Lichens

Mountain ecosystem

## ABSTRACT

Over the past century, atmospheric nitrogen deposition ( $N_{\text{dep}}$ ) has increased across the western United States due to agricultural and urban development, resulting in degraded ecosystem quality. Regional patterns of  $N_{\text{dep}}$  are often estimated by coupling direct measurements from large-scale monitoring networks and atmospheric chemistry models, but such efforts can be problematic in the western US because of complex terrain and sparse sampling. This study aimed not only to understand  $N_{\text{dep}}$  patterns in mountainous ecosystems but also to investigate whether isotope values of lichens and throughfall deposition can be used to determine  $N_{\text{dep}}$  sources, and serve as an additional tool in ecosystem health assessments. We measured  $N_{\text{dep}}$  amounts and  $\delta^{15}\text{N}$  in montane conifer forests of the Greater Yellowstone Ecosystem using canopy throughfall and bulk monitors and lichens. In addition, we examined patterns of C:N ratios in lichens as a possible indicator of lichen physiological condition. The isotopic signature of  $\delta^{15}\text{N}$  of  $N_{\text{dep}}$  helps to discern emission sources, because  $\delta^{15}\text{N}$  of  $\text{NO}_x$  from combustion tends to be high (-5 to 25‰) while  $\text{NH}_x$  from agricultural sources tends to be comparatively low (-40 to -10‰). Summertime  $N_{\text{dep}}$  increased with elevation and ranged from 0.26 to 1.66 kg ha<sup>-1</sup>.  $N_{\text{dep}}$  was higher than expected in remote areas. The  $\delta^{15}\text{N}$  values of lichens were typically -15.3 to -10‰ suggesting agriculture as a primary emission source of deposition. Lichen  $\%N$ ,  $\delta^{15}\text{N}$  and C:N ratios can provide important information about  $N_{\text{dep}}$  sources and patterns over small spatial scales in complex terrain.

© 2019 Published by Elsevier B.V.

\* Corresponding author.

E-mail address: [ahoffm12@uwyo.edu](mailto:ahoffm12@uwyo.edu) (A.S. Hoffman).

## 1. Introduction

Total reactive atmospheric nitrogen deposition ( $N_{\text{dep}}$ ) increased threefold globally during the 20th century, leading to acidification of surface water and soils, increased leaching of cations, and changes in plant communities through altered competitive relationships (Bobbink et al., 2010; Galloway et al., 2004; Vitousek et al., 1997). Mountainous ecosystems are particularly susceptible to  $N_{\text{dep}}$  because they are typically low in nutrients due to poor soils and have low thresholds for  $N_{\text{dep}}$  before water quality decreases and plant communities are impacted (Burns, 2004; Lieb et al., 2011; Williams et al., 2017).

Global increases in  $N_{\text{dep}}$  are attributed to expansion of intensively managed agriculture, which is the principle source of reduced atmospheric N ( $\text{NH}_x$ ), and transportation and industrial activities that release nitrogen oxides ( $\text{NO}_x$ ) through high temperature combustion (Galloway et al., 2004). Broad regional drivers of  $N_{\text{dep}}$  include climate and distance to point and non-point sources of N.  $N_{\text{dep}}$  is often greatest at high elevations where greater precipitation increases deposition rates through aerosol scavenging and dissolution of  $\text{NH}_3$  and  $\text{HNO}_3$  (Beem et al., 2010; Clow et al., 2015; Weathers et al., 2000).  $N_{\text{dep}}$  is positively correlated with ion concentrations in precipitation, which are driven by proximity to emissions sources, and total precipitation (Kopáček et al., 2012). However, it is unclear to what extent these patterns are observed across complex landscapes with diverse non-point sources. Montane areas generally receive more deposition than adjacent lowland, but heterogeneous topography creates complex interactions between wind patterns, slope, aspect, emissions sources and chemistry causing high variability across small spatial scales, such as between adjacent hillslopes (Giannoni et al., 2013; Kirchner et al., 2014; Kopáček et al., 2012; Weathers et al., 2006).

Determining sources and patterns of  $N_{\text{dep}}$  in montane areas is required to devise policies and management actions that will minimize impacts to sensitive ecosystems and to understand small scale patterns and mechanisms that can improve modeling at larger scales. Air quality studies have led to tighter standards for  $\text{NO}_x$  emissions, which is reflected in decreasing patterns of  $\text{NO}_3^-$  deposition at national monitoring sites (Lloret and Valiela, 2016). Nitrogen emission sources can be traced using  $^{15}\text{N}/^{14}\text{N}$  isotope ratios at natural abundance levels. The  $\delta^{15}\text{N}$  of most fertilizers and animal waste is  $-0\text{‰}$ , but the observed discrimination for the  $\text{NH}_4 - \text{NH}_3$  equilibrium and subsequent  $\text{NH}_3$  volatilization are 20 to 27‰, and 29‰, respectively, causing  $N_{\text{dep}}$  derived from agricultural sources to have low  $\delta^{15}\text{N}$  ( $-40$  to  $-10\text{‰}$ ) (Ti et al., 2018). In contrast, emissions from combustion sources have comparatively high  $\delta^{15}\text{N}$  ( $-5$  to  $25\text{‰}$ ), reflecting the fuel source (Elliott et al., 2007; Felix et al., 2014, 2017; Felix and Elliott, 2014).

Lichens are useful indicators of localized  $N_{\text{dep}}$  because they absorb nutrients out of the atmosphere so their nitrogen content and stable isotope composition can record fine scale pollution patterns (Fenn et al., 2007; Glavich and Geiser, 2008; Root et al., 2015). Lichen collections are a cost-effective method to assess nitrogen pollution, particularly in remote areas that are difficult to access with monitoring equipment. Several studies have documented comparatively high %N concentrations in lichens close to pollution sources (Boltersdorf and Werner, 2014; Fenn et al., 2007; McMurray et al., 2013). However, the mechanisms by which lichens incorporate N could be influenced by both the amount of N deposition and climate. The relationship between %N in lichens and  $N_{\text{dep}}$  could be more complex than previous linear models describe, in part because %N content is influenced by climatic variables such as the type and amount of precipitation and relative humidity (McMurray et al., 2015; Root et al., 2013), as well as total rates and speciation of  $N_{\text{dep}}$ , and because different species of lichens respond to varying rates of  $N_{\text{dep}}$  under different climate regimes, at rates that can vary from weeks to years. (Fremstad et al., 2005; Johansson et al., 2010; Munzi et al., 2019).

In this study we measured  $N_{\text{dep}}$  using ion exchange resin (IER) collectors and collected individual lichens to better understand how they

respond to  $N_{\text{dep}}$  and climate gradients, with the goal of estimating amounts and impacts of  $N_{\text{dep}}$ . Our objectives were to 1) understand how elevation, precipitation, and proximity to emission sources, influence  $N_{\text{dep}}$  patterns in the Greater Yellowstone Ecosystem (GYE), 2) correlate measured deposition to % N in lichen thalli and, 3) to investigate the use of  $\delta^{15}\text{N}$  from lichen and  $N_{\text{dep}}$  (IER monitors) as a means of source identification. We expected  $N_{\text{dep}}$  to be higher at higher elevation sites and at sites closer to regional agricultural N emission sources in the western GYE (Beem et al., 2010; Benedict et al., 2013a; Prenni et al., 2014). Additionally, we expected lichens to reflect  $N_{\text{dep}}$  amounts and sources, despite the high expected variability among individual lichens than in the more typical bulk lichen collections. Finally, previous work shows there are large inputs of  $N_{\text{dep}}$  from agriculture to the west in the Snake River Plain and urban emissions from UT (Benedict et al., 2013b), while oil and gas activity (McMurray et al., 2013), vehicle emissions, and long distance transport (Lee et al., 2016; Zhang et al., 2018) also contribute to  $N_{\text{dep}}$ .

## 2. Methods

### 2.1. Study sites

We established three elevation transects and one transect with increasing distance from the Snake River Plain (SRP) across the GYE to evaluate variation in N sources and deposition patterns across the region (Fig. 1, Table 1). The GYE, with the iconic Yellowstone National Park (YNP) at its center, is one of the largest intact temperate ecosystems on earth. The GYE is downwind from long range transport of N,  $\text{NH}_3$  emissions from more local agriculture to the west, and  $\text{NO}_x$  emissions to the south and southwest (Benedict et al., 2013a; Lee et al., 2016). Previous studies have voiced concern over increasing  $N_{\text{dep}}$  in the GYE but no previous study has measured  $N_{\text{dep}}$  in transects across the interior of the GYE. The study area included several mountain ranges with diverse climate patterns and distances to emissions that provided the opportunity to study how  $N_{\text{dep}}$  patterns are mediated by regional patterns of climate and elevation as well as local topography and weather. The SRP, west of the GYE in southern Idaho is a concentrated area of irrigated agriculture, dairy farming and aquaculture, which contribute to high emissions in the SRP (Benedict et al., 2013a; National Emissions Inventory, 2014).

The elevation transect at Grand Targhee Ski Resort (GT) was 15 km west of the SRP and is influenced by agricultural emissions (Benedict et al., 2013a). The west-facing transect included four sites that ranged from 2317 to 2888 m elevation, with mean annual precipitation ranging from 557 to 638 mm (Thornton et al., 2014). The elevation transect at Jackson Hole Mountain Resort (JH) included four sites that ranged in elevation from 1967 to 3029 m, with mean annual precipitation ranging from 540 to 652 mm (Thornton et al., 2014). This southeast-facing transect is influenced relatively more by urban N emissions from the ski resort as well as the city of Jackson, WY due to inversions and upslope winds. The elevation transect at Avalanche Peak (AP) was in a remote area of YNP and included three sites ranging in elevation from 2537 to 2880 m, with mean annual precipitation ranging from 547 to 565 mm (Thornton et al., 2014). The distance transect (Dist) was set up to vary with distance downwind from agriculture in the SRP, with sites at 1, 15, 52 and 112 km from the SRP. The elevations of these sites ranged from 1940 m to 2334 m, and mean annual precipitation ranged from 392 to 691 mm (Thornton et al., 2014).

### 2.2. Field $N_{\text{dep}}$ collection and chemical analyses

We used ion exchange resin (IER) collectors to measure  $N_{\text{dep}}$  in the GYE from June 2016 to September 2016. At each site, we placed 3 bulk IER collectors in open areas, 6 throughfall IER collectors under spruce (*P. engelmannii*) or subalpine fir (*A. lasiocarpa*) canopies, and one capped IER tube, which was a field blank to control for leaching from

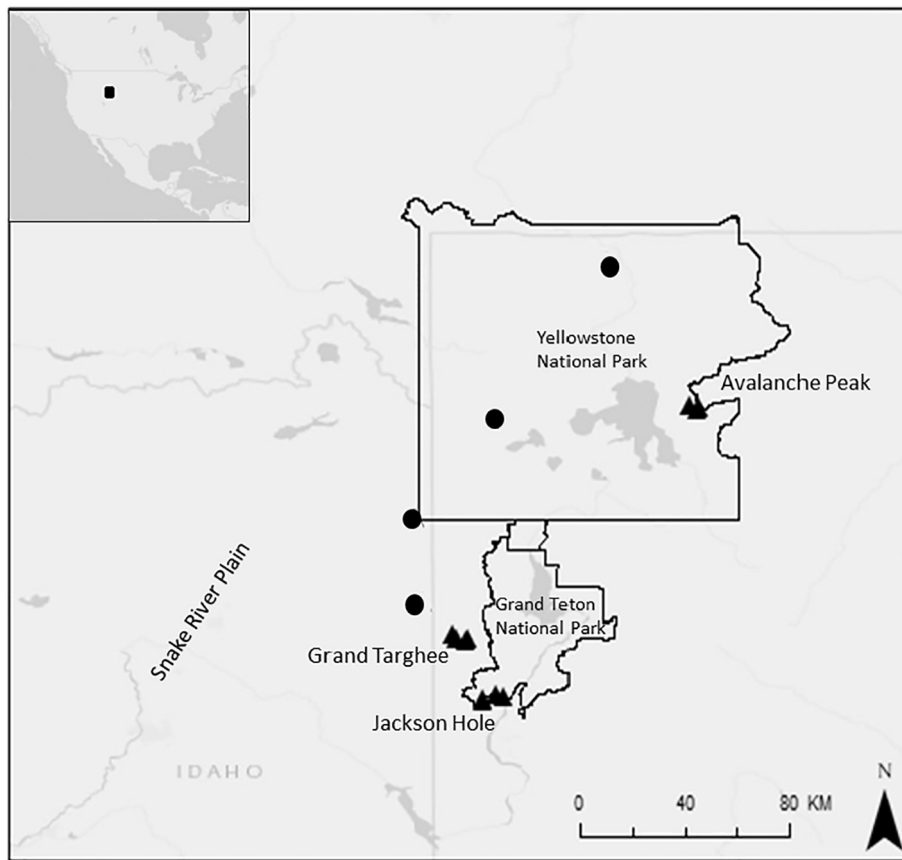


**Fig. 1.** A map of the Greater Yellowstone Ecosystem with study sites at elevation transects at Grand Targhee Ski Resort, Jackson Hole Mountain Resort and Avalanche Peak, represented by triangles and study sites that are part of the transect with increasing distance from the Snake River Plain represented by circles.

IER. The collectors were made up of a mixed bed IER column attached to a funnel with a diameter of 22.86 cm and mounted on a fence post so that the base of the collecting funnel was about 1 m off the ground. We assembled collectors following the protocol described by Fenn and Poth (2004), which were shown to be effective for accurately measuring  $N_{dep}$  when compared with other measurements (Fenn and Poth, 2004). Fifty grams of resin were placed into each tube and then distilled water was poured through the tubes to remove any trace contaminants. The collectors were fitted with wire prongs around the rim to prevent contamination from perching birds.

Each IER column collected from the field was extracted with 200 mL 2 M KCl in the lab. The extracts were analyzed for  $NH_4$  and  $NO_3^-$  concentrations using colorimetry (Lachat Quickchem 8500) (Hofer, 2003; Knepel, 2003). Concentrations were used to estimate area-based N deposition amounts over the summer collection period ( $kg\ N\ ha^{-1}$ ) based on the size of the funnel and volume of the extract. Total  $NH_4$  and  $NO_3^-$  mass measured in field blanks were subtracted from values measured in collector deposition to correct for possible leaching. These collectors measure total deposition over the time period that they were in the field. Because it would be impossible to establish and

**Table 1**

The locations of ion exchange resin collectors and lichen collections in this study, as well as the elevation, modeled precipitation and dominant tree species at each site.

| Site             | Latitude  | Longitude   | Elevation (m) | Summer precipitation (mm) | Annual precipitation as rain (mm) | Annual days of precipitation | Dominant tree species                                |
|------------------|-----------|-------------|---------------|---------------------------|-----------------------------------|------------------------------|--|
| Avalanche Peak 1 | 44.486117 | -110.170661 | 2537          | 77                        | 557                               | 282                          | <i>Abies lasiocarpa</i>                              |
| Avalanche Peak 2 | 44.471513 | -110.143398 | 2612          | 81                        | 547                               | 279                          | <i>Abies lasiocarpa</i>                              |
| Avalanche Peak 3 | 44.479575 | -110.13975  | 2880          | 84                        | 565                               | 272                          | <i>Abies lasiocarpa</i>                              |
| Grand Targhee 1  | 43.788973 | -110.98004  | 2317          | 62                        | 638                               | 288                          | <i>Abies lasiocarpa</i>                              |
| Grand Targhee 2  | 43.780154 | -110.96514  | 2452          | 70                        | 664                               | 287                          | <i>Abies lasiocarpa</i>                              |
| Grand Targhee 3  | 43.768944 | -110.931608 | 2683          | 70                        | 665                               | 283                          | <i>Abies lasiocarpa</i>                              |
| Grand Targhee 4  | 43.78068  | -110.92562  | 2888          | 72                        | 557                               | 260                          | <i>Abies lasiocarpa</i> , <i>Pinus albicaulis</i>    |
| Jackson Hole 1   | 43.605985 | -110.805694 | 1967          | 70                        | 568                               | 299                          | <i>Pinus contorta</i> , <i>Pseudotsuga menziesii</i> |
| Jackson Hole 2   | 43.609823 | -110.832022 | 2535          | 82                        | 652                               | 290                          | <i>Abies lasiocarpa</i>                              |
| Jackson Hole 3   | 43.589563 | -110.875071 | 2881          | 84                        | 540                               | 264                          | <i>Abies lasiocarpa</i> , <i>Pinus albicaulis</i>    |
| Jackson Hole 4   | 43.594867 | -110.878528 | 3029          | 84                        | 571                               | 266                          | <i>Abies lasiocarpa</i> , <i>Picea engelmannii</i>   |
| Distance 1       | 43.889776 | -111.083645 | 2094          | 55                        | 652                               | 298                          | <i>Pseudotsuga menziesii</i>                         |
| Distance 2       | 44.143361 | -111.108935 | 2048          | 44                        | 691                               | 304                          | <i>Pinus contorta</i>                                |
| Distance 3       | 44.443467 | -110.803421 | 2334          | 80                        | 598                               | 290                          | <i>Picea engelmannii</i> , <i>Pinus contorta</i>     |
| Distance 4       | 44.922004 | -110.454921 | 1940          | 91                        | 392                               | 298                          | <i>Pseudotsuga menziesii</i>                         |

retrieve all collectors on the same start and end dates, time in the field ranged from 84 to 134 days so deposition was standardized to a 100-day period during summer. Total phosphorus was measured in the twenty samples with the highest  $\text{NH}_4$  concentrations using inductively coupled plasma–optical emission spectrometry (ICP–OES, PerkinElmer Optima 8300) to check for contamination from bird excrement. Phosphorus concentrations ranged from  $0.211 \text{ mg L}^{-1}$  to  $20.81 \text{ mg L}^{-1}$ , corresponding to deposition rates of  $0.01$  to  $0.91 \text{ kg ha}^{-1}$ . These values were within natural deposition ranges (Decina et al., 2018), so we determined there was no contamination from perching birds.

We measured  $\delta^{15}\text{N}$  of dissolved  $\text{NO}_3^-$  and  $\text{NH}_4^+$  at each site to understand sources of  $\text{N}_{\text{dep}}$ .  $\delta^{15}\text{N}$  values for bulk and throughfall collections at each site were analyzed separately to detect whether canopies were processing N or just collecting dry  $\text{N}_{\text{dep}}$  (Heaton et al., 1997). Stable isotope ratios were calculated relative to the atmospheric  $\text{N}_2$  standard using delta notation:

$$\delta\text{N} (\text{‰}) = \left( \frac{R_{\text{sample}}}{R_{\text{standard}}} - 1 \right) \times 1000 \quad (1)$$

where R was the ratio of the heavy to light isotope in the sample or standard. The  $\text{NH}_4$  from IER extracts were collected onto filters using the ammonia diffusion method (Holmes et al., 1998). Samples were diluted to a concentration of approximately  $0.5 \text{ mg NH}_4\text{-N L}^{-1}$  and  $150 \text{ mL}$  of each dilution was placed in a  $250 \text{ mL}$  bottle, where  $0.45 \text{ g}$  of  $\text{MgO}$  were added to facilitate conversion of  $\text{NH}_4^+$  to  $\text{NH}_3$  gas and diffusion into the headspace. We placed filter packs made of  $25 \mu\text{L}$  of  $3 \text{ M H}_2\text{SO}_4$  on pre-combusted  $1 \text{ cm}$  GF/D filters sealed between  $2 \text{ cm}$  Teflon filters to trap the  $\text{NH}_3$  gas in the headspace. Bottles were tightly sealed and placed on a shaker bench for 15 days at room temperature to allow for diffusion of  $\text{NH}_3$  into the headspace and collection onto the filters. The filters were combusted in an elemental analyzer coupled to an isotope ratio mass spectrometer (EA-IRMS, Thermo Finnigan Delta Plus XP, Carlo Erba 1110 Elemental Analyzer). Standards of  $0.25$ ,  $0.50$  and  $1.00 \text{ mg N L}^{-1}$  were used to quantify observed discrimination during the conversion and collection of  $\text{NH}_3$ .

We measured the  $\delta^{15}\text{N}\text{-NO}_3^-$  isotope ratios by converting  $\text{NO}_3^-$  in IER extracts to  $\text{N}_2\text{O}$  using the microbial denitrifier method (Sigman et al., 2001). *Pseudomonas chlororaphis* were incubated in stock media solution for 2 days. The cultures were divided into  $50 \text{ mL}$  tubes and centrifuged for 12 min at  $7200 \text{ rpm}$  to form a pellet. The supernatant was decanted and  $15 \text{ mL}$  of  $\text{NO}_3^-$ -free media was mixed into each tube. The tubes were vortexed to form a pellet and the supernatant was decanted. Rinsing with  $\text{NO}_3^-$  free media was repeated three times to remove all nitrogen used to grow bacteria. The bacteria from all centrifuge tubes were then combined in  $30 \text{ mL}$  of  $\text{NO}_3^-$ -free media and  $2 \text{ mL}$  of the bacteria solution was pipetted into 12 vials. The vials were flushed with  $\text{N}_2$  gas for 1 h and then placed on a heated shaker for 12 h. Two milliliter of each sample were added to the vials containing the bacteria. Samples were diluted to approximately  $20 \mu\text{mol NO}_3^-$  before injection. The vials were left for 1 h on the shaker bench to allow bacteria to convert  $\text{NO}_3^-$  to  $\text{N}_2\text{O}$ , before  $\text{NaOH}$  was added to kill bacterial cells and stop the reaction. The  $\text{N}_2\text{O}$  gas was collected from the headspace of the vials and analyzed using gas chromatography (GC)-IRMS (Thermo Scientific Delta V). We included and analyzed four  $\text{NO}_3^-$  standards with each batch of samples.

### 2.3. Lichen collections and analyses

Where possible, at each site we collected 6 specimens of *Usnea lapponica* and *Letharia vulpina* that were co-located on conifer trees where throughfall IER collectors were placed. These two species of lichens are ubiquitous throughout the study area, but *U. lapponica* typically has higher N content (Geiser et al., 2010; McMurray et al., 2013). All lichens were collected  $>1 \text{ m}$  off the ground, hand cleaned of debris, oven dried for 24 h at  $40 \text{ }^\circ\text{C}$ , and homogenized. A sub-sample was

then loaded into a tin and combusted, and %N, %C,  $\delta^{15}\text{N}$ , and  $\delta^{13}\text{C}$  were measured using EA-IRMS.

### 2.4. Statistical analyses

We used R to perform all statistical analyses (R Core Team, 2018). We plotted  $\text{IER N}_{\text{dep}}$ , and  $\delta^{15}\text{N}$ , and lichen %N and  $\delta^{15}\text{N}$  against elevation for each transect and used analysis of variance and TukeyHSD post hoc tests to determine significant differences between sites using  $\alpha \leq 0.05$ . Additionally, we used linear regression to test the relationship between  $\text{IER N}_{\text{dep}}$  and lichen %N or C:N and  $\text{IER } \delta^{15}\text{N}$  and lichen  $\delta^{15}\text{N}$ .

## 3. Results

### 3.1. Ion exchange resin collectors

We collected 72 throughfall and 38 bulk IER samples across 15 sites categorized into four transects. Concentrations of  $\text{NO}_3^-$  ranged from  $0.05$  to  $6.01 \text{ mg N L}^{-1}$  and concentrations of  $\text{NH}_4$  ranged from  $0.032$  to  $21.8 \text{ mg N L}^{-1}$ . The method detection limit for  $\text{NO}_3^-$  was  $0.005 \text{ mg N L}^{-1}$  and the detection limit for  $\text{NH}_4$  was  $0.02 \text{ mg N L}^{-1}$ . The standard deviation of replicate samples was  $0.008$  for  $\text{NO}_3^-$  and  $0.117$  for  $\text{NH}_4$ . The standard deviation of known standards was  $0.15 \text{ mg N L}^{-1}$  for  $\text{NO}_3^-$  and  $0.06 \text{ mg N L}^{-1}$  for  $\text{NH}_4$ . The field blanks averaged  $0.007 \pm 0.0002 \text{ mg NO}_3^- \text{-N}$  and  $0.168 \pm 0.018 \text{ mg NH}_4\text{-N}$ .

After subtraction of field blanks, the mean ( $\pm 95\%$  CI) bulk  $\text{N}_{\text{dep}}$  for the summer across all sites was  $0.80 \pm 0.14 \text{ kg N ha}^{-1}$  ( $0.63 \text{ kg NH}_4\text{-N ha}^{-1}$  and  $0.17 \text{ kg NO}_3^- \text{-N ha}^{-1}$ ) and mean throughfall  $\text{N}_{\text{dep}}$  was  $1.25 \pm 0.24 \text{ kg ha}^{-1}$  ( $1.05 \text{ kg NH}_4\text{-N ha}^{-1}$  and  $0.20 \text{ kg NO}_3^- \text{-N ha}^{-1}$ ). The lowest bulk  $\text{N}_{\text{dep}}$  was  $0.26 \text{ kg N ha}^{-1}$  measured at AP1, but there was only one replicate (Table 2). AP2 had the second lowest bulk  $\text{N}_{\text{dep}}$  with  $0.38 \pm 0.38 \text{ kg N ha}^{-1}$  ( $0.30 \text{ kg NH}_4\text{-N ha}^{-1}$  and  $0.08 \text{ kg NO}_3^- \text{-N ha}^{-1}$ ) (Table 2). AP3 had the highest bulk  $\text{N}_{\text{dep}}$  with  $1.66 \pm 0.35 \text{ kg N ha}^{-1}$  ( $1.26 \text{ kg NH}_4\text{-N ha}^{-1}$  and  $0.40 \text{ kg NO}_3^- \text{-N ha}^{-1}$ ) (Table 2). Sites at higher elevations had higher  $\text{N}_{\text{dep}}$ . However, this trend was only significant ( $p < 0.05$ ) at the AP transect (Fig. 2). Throughfall  $\text{N}_{\text{dep}}$  was significantly higher ( $p < 0.05$ ) than bulk  $\text{N}_{\text{dep}}$  at the GT and JH transects (Fig. 2). The  $\text{N}_{\text{dep}}$  along the distance transect did not have a clear trend and the highest amount of bulk  $\text{N}_{\text{dep}}$  occurred at the site furthest from the SRP, but differences between sites are not significant. Nitrogen from  $\text{NH}_4$  made up the majority of  $\text{N}_{\text{dep}}$  at all sites, with an average ratio for  $\text{NH}_4\text{-N} : \text{NO}_3^- \text{-N}$  of  $9.3:1$  in bulk deposition and  $11.8:1$  in throughfall deposition (Table 2).  $\delta^{15}\text{N}\text{-NH}_4$  was between  $-5.7$  and  $2.7\%$ , except for in bulk deposition at JH2 and Dist3 and Dist4, which were  $8.9$ ,  $13.8$  and  $15.8\%$  respectively, and the throughfall deposition at GT1, which was  $6.2\%$  (Table 2). The standard deviation of  $\delta^{15}\text{N}\text{-NH}_4$  for known standards was  $0.22\%$ .  $\delta^{15}\text{N}\text{-NO}_3^-$  generally was between  $-12.5\%$  and  $-0.7\%$ , but there were two high throughfall values of  $20.6\%$  and  $11.1\%$  at the JH4 and Dist4 sites, respectively (Table 2). The standard deviation of  $\delta^{15}\text{N}\text{-NO}_3^-$  for known standards was  $0.4\%$ .

### 3.2. Lichen analyses

We collected 86 *U. lapponica* and 104 *L. vulpina* across the four transects. The average standard deviation of duplicate samples was  $0.03$  for %N,  $0.15$  for %C,  $0.06$  for  $\delta^{15}\text{N}$ , and  $0.04$  for  $\delta^{13}\text{C}$ . For check standards, the average deviation from known values was  $0.08$  for %N,  $0.87$  for %C,  $0.06$  for  $\delta^{15}\text{N}$  was, and  $0.09$  for  $\delta^{13}\text{C}$ . Across all sites, individual *U. lapponica* samples ranged from  $0.70$  to  $2.54\%$  N with a mean of  $1.53\%$  N and a standard deviation of  $0.43$ , while *L. vulpina* ranged from  $0.71$  to  $2.13\%$  N with a mean of  $1.32\%$  N and a standard deviation of  $0.32$ . Individual lichens often had high variation within sites (Table 3).

*U. lapponica* and *L. vulpina* %N had similar trends across sites, but *U. lapponica* had higher %N than *L. vulpina* (Fig. 3). Lichen %N at the GT transect increased with elevation from  $1.14 \pm 0.15\%$  to  $1.54 \pm 0.13\%$  in *L. vulpina*. Lichen %N also increased with elevation at the JH transect,



**Table 2**

The number of collectors, total inorganic N (mean  $\pm$  95% CI), average ratios of  $\text{NH}_4\text{-N}$  to  $\text{NO}_3\text{-N}$  in deposition, and  $\delta^{15}\text{N}$  isotope ratios in bulk and throughfall ion exchange resin collectors at four transects throughout the Greater Yellowstone Ecosystem. Some  $\delta^{15}\text{N}$  ratios are missing because there was not enough sample to analyze or because of instrument errors.

| Site  | Count |    | Inorganic N ( $\text{kg ha}^{-1}$ ) |                 | $\text{NH}_4\text{:NO}_3$ ratio |      | $\delta^{15}\text{N}\text{-NO}_3$ (‰) |       | $\delta^{15}\text{N}\text{-NH}_4$ (‰) |      |
|-------|-------|----|-------------------------------------|-----------------|---------------------------------|------|---------------------------------------|-------|---------------------------------------|------|
|       | Bulk  | tf | Bulk                                | tf              | Bulk                            | tf   | Bulk                                  | tf    | Bulk                                  | tf   |
| AP1   | 1     | 2  | 0.26                                | $0.45 \pm 0.54$ | 13.1                            | 9.6  |                                       | -2.2  |                                       | -5.5 |
| AP2   | 3     | 6  | $0.38 \pm 0.38$                     | $1.15 \pm 0.45$ | 26.3                            | 4.5  | -4.4                                  | -4.4  | -3.6                                  | -3.3 |
| AP3   | 2     | 2  | $1.66 \pm 0.35$                     | $1.51 \pm 1.2$  | 3.2                             | 3.0  | -2.9                                  | -12.5 | -2.7                                  | -1.9 |
| GT1   | 2     | 6  | $0.65 \pm 0.79$                     | $0.99 \pm 0.58$ | 11.1                            | 20.2 |                                       | -1.8  | -4.7                                  | 6.2  |
| GT2   | 2     | 6  | $0.74 \pm 0.42$                     | $2.11 \pm 0.86$ | 26.6                            | 43.0 | -4.0                                  | -10.3 | -3.6                                  |      |
| GT3   | 2     | 4  | $0.79 \pm 0.46$                     | $1.79 \pm 0.31$ | 8.4                             | 7.7  | -4.1                                  | -8.8  | 1.1                                   | -0.6 |
| GT4   | 3     | 6  | $1.07 \pm 0.43$                     | $1.03 \pm 0.54$ | 2.4                             | 3.2  | -4.2                                  | -6.9  | -3.5                                  | -1.1 |
| JH1   | 3     | 5  | $0.46 \pm 0.26$                     | $1.04 \pm 0.19$ | 4.9                             | 4.2  | -4.4                                  | -10.7 | -3.1                                  | -0.5 |
| JH2   | 3     | 6  | $0.81 \pm 0.29$                     | $1.46 \pm 0.31$ | 4.6                             | 9.6  |                                       | -5.0  | 8.9                                   | 2.7  |
| JH3   | 3     | 6  | $0.92 \pm 0.46$                     | $1.13 \pm 0.66$ | 25.0                            | 13.4 | -4.4                                  | -5.2  | -1.7                                  | -3.0 |
| JH4   | 3     | 6  | $0.88 \pm 0.24$                     | $1.54 \pm 0.55$ | 3.0                             | 20.2 | -4.5                                  | 20.6  | -2.3                                  | -2.8 |
| Dist1 | 3     | 4  | $0.56 \pm 0.92$                     | $1.23 \pm 0.41$ | 1.1                             | 4.0  | -0.7                                  | -2.6  | -3.0                                  | -2.5 |
| Dist2 | 3     | 6  | $0.98 \pm 0.41$                     | $0.41 \pm 0.45$ | 3.6                             | 2.6  | -3.6                                  | -4.2  | -4.1                                  | -3.0 |
| Dist3 | 3     | 1  | $0.61 \pm 0.29$                     | 0.99            | 56.0                            | 6.6  | -5.1                                  | -6.5  | 13.8                                  | -1.9 |
| Dist4 | 2     | 6  | $1.17 \pm 0.01$                     | $1.46 \pm 0.58$ | 5.3                             | 8.3  | -5.4                                  | 11.1  | 15.8                                  | -1.4 |

from  $1.18 \pm 0.19\%$  to  $2.06 \pm 0.46\%$  in *U. lapponica* and  $0.96 \pm 0.13\%$  to  $1.57 \pm 0.23\%$  in *L. vulpina*, although the biggest increase in %N came between the first and second sites (Fig. 3). Lichen %N at sites along the AP transect were relatively constant with %N in lichens ranging between  $1.18 \pm 0.10\%$  and  $1.32 \pm 0.25\%$ , except at the lowest site where *U. lapponica* averaged  $1.81 \pm 0.24\%$  N (Fig. 3). At sites along the distance transect, lichen %N did not have a clear trend and %N ranged from  $1.14 \pm 0.16\%$  to  $2.02 \pm 0.31\%$  (Fig. 3). Lichen  $\delta^{15}\text{N}$  were generally low across sites, mostly ranging between  $-16\%$  to  $-10\%$ . However, the JH transect had a few sites with values that were higher than  $-10\%$ , averaging  $-7.6 \pm 4.1\%$  and  $-6.0 \pm 1.3\%$  in *L. vulpina* at the middle elevation sites (JH2 and JH3), and  $-2.8 \pm 6.7\%$  in *U. lapponica* at JH2 (Fig. 4).

### 3.3. Ion exchange resin collector and lichen comparisons

Throughfall  $N_{\text{dep}}$  was positively correlated with %N in *L. vulpina* ( $p = 0.0001$ ), but the relationship was weak ( $R^2 = 0.19$ , Fig. 5). Throughfall  $N_{\text{dep}}$  also was positively correlated with C:N ratios in both *L. vulpina* ( $p < 0.0001$ ) and *U. lapponica* ( $p = 0.04$ ), although the relationships

were also weak ( $R^2 = 0.22$  and  $R^2 = 0.06$ , respectively). Lichen  $\delta^{15}\text{N}$  values were not correlated with  $\delta^{15}\text{N}$  of  $\text{NH}_4$ ,  $\text{NO}_3$ , or concentration weighted means of  $\delta^{15}\text{N}$  of  $\text{NH}_4$  and  $\text{NO}_3$  for bulk or throughfall  $N_{\text{dep}}$  ( $p > 0.05$ ).

## 4. Discussion

We collected 104 *L. vulpina* at 15 sites and 86 *U. lapponica* at 14 sites across the GYE. *U. lapponica* were difficult to find at high elevation sites (JH4, GT3, GT4, and AP3), with only 5 collections across those sites. We also measured deposition in 38 bulk collectors and 72 throughfall collectors across 15 sites in the GYE. Generally, lichen %N and bulk deposition increased with elevation, but there was large variation and these relationships were mostly not significant. Throughfall deposition increased with elevation at the AP transect, but had higher variation within sites (Fig. 2, Table 2). Ratios of  $\text{NH}_4\text{-N}$  to  $\text{NO}_3\text{-N}$  and  $\delta^{15}\text{N}$  isotope ratios in bulk and throughfall deposition and lichens indicated predominantly agricultural sources of N.  $N_{\text{dep}}$  was highest at sites in remote parts of the northern GYE that do not have significant local sources,

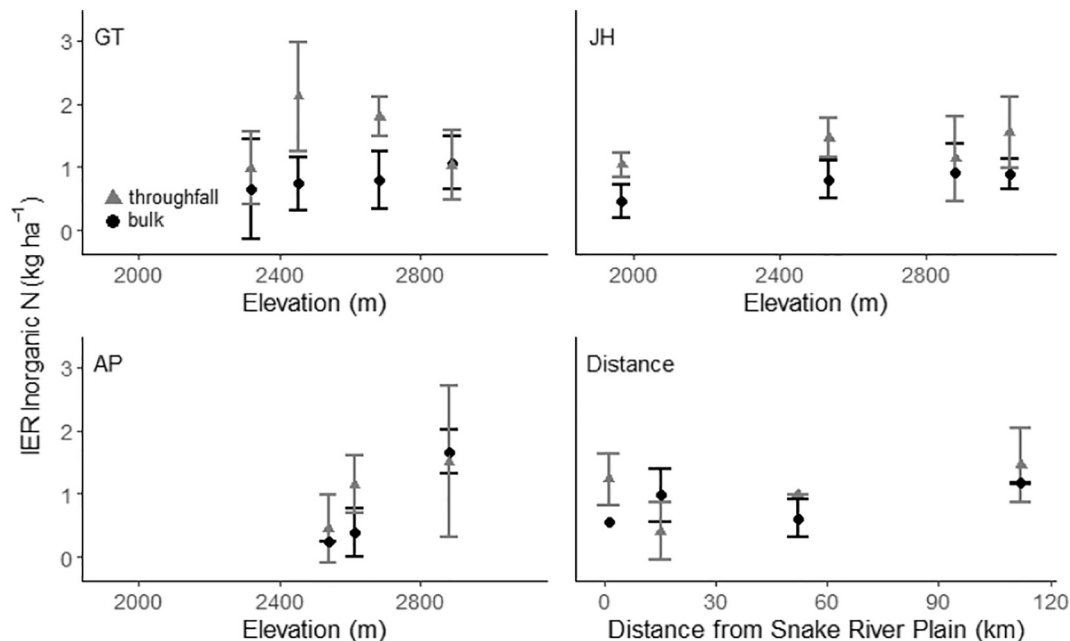


**Fig. 2.** Mean ( $\pm 95\%$  CI) nitrogen deposition measured from June to September 2016 in ion exchange resin (IER) collectors established at four transects across the Greater Yellowstone Ecosystem near Grand Targhee Ski Resort (GT), Jackson Hole Mountain Resort (JH), Avalanche Peak (AP), and a transect with increasing distance from the Snake River Plain.

**Table 3**  
The number of lichen collections and average lichen %N (mean  $\pm$  95% CI), lichen  $\delta^{15}\text{N}$  (mean  $\pm$  95% CI), and lichen C:N ratio of *U. lapponica* and *L. vulpina* lichens collected at four transects across the Greater Yellowstone Ecosystem. At high elevation sites, *U. lapponica* were uncommon so there were missing collections and lower sample sizes.

| Site  | Count             |                     | %N                |                     | $\delta^{15}\text{N}$ (‰) |                     | C:N ratio         |                     |
|-------|-------------------|---------------------|-------------------|---------------------|---------------------------|---------------------|-------------------|---------------------|
|       | <i>L. vulpina</i> | <i>U. lapponica</i> | <i>L. vulpina</i> | <i>U. lapponica</i> | <i>L. vulpina</i>         | <i>U. lapponica</i> | <i>L. vulpina</i> | <i>U. lapponica</i> |
| AP1   | 6                 | 4                   | 1.31 $\pm$ 0.22   | 1.81 $\pm$ 0.24     | -12.7 $\pm$ 1.4           | -13.9 $\pm$ 1.0     | 36.5              | 25.9                |
| AP2   | 6                 | 6                   | 1.18 $\pm$ 0.10   | 1.30 $\pm$ 0.21     | -15.2 $\pm$ 1.3           | -15.3 $\pm$ 1.9     | 39.7              | 35.9                |
| AP3   | 6                 | 0                   | 1.32 $\pm$ 0.25   |                     | -13.0 $\pm$ 1.2           |                     | 36.2              |                     |
| GT1   | 11                | 12                  | 1.14 $\pm$ 0.15   | 1.25 $\pm$ 0.34     | -14.9 $\pm$ 0.9           | -13.7 $\pm$ 1.5     | 40.0              | 37.9                |
| GT2   | 9                 | 12                  | 1.29 $\pm$ 0.20   | 1.39 $\pm$ 0.34     | -11.8 $\pm$ 0.9           | -11.4 $\pm$ 1.7     | 35.5              | 33.2                |
| GT3   | 13                | 2                   | 1.54 $\pm$ 0.13   | 1.65 $\pm$ 0.04     | -10.8 $\pm$ 1.0           | -10.2 $\pm$ 0.6     | 29.4              | 27.3                |
| GT4   | 6                 | 2                   | 1.48 $\pm$ 0.25   | 1.76 $\pm$ 0.40     | -10.3 $\pm$ 2.0           | -11.8 $\pm$ 0.4     | 31.7              | 26.1                |
| JH1   | 8                 | 12                  | 0.96 $\pm$ 0.13   | 1.18 $\pm$ 0.19     | -11.6 $\pm$ 1.0           | -13.6 $\pm$ 1.1     | 48.7              | 39.2                |
| JH2   | 7                 | 8                   | 1.45 $\pm$ 0.26   | 2.06 $\pm$ 0.46     | -7.6 $\pm$ 4.1            | -2.8 $\pm$ 6.7      | 32.0              | 22.8                |
| JH3   | 3                 | 6                   | 1.57 $\pm$ 0.23   | 1.74 $\pm$ 0.22     | -6.0 $\pm$ 1.3            | -11.9 $\pm$ 1.4     | 29.8              | 26.0                |
| JH4   | 5                 | 1                   | 1.35 $\pm$ 0.22   | 1.71                | -11.8 $\pm$ 2.4           | -13.2               | 34.7              | 26.7                |
| Dist1 | 6                 | 6                   | 1.52 $\pm$ 0.32   | 2.02 $\pm$ 0.31     | -11.5 $\pm$ 0.4           | -11.7 $\pm$ 1.3     | 32.1              | 22.7                |
| Dist2 | 6                 | 3                   | 1.44 $\pm$ 0.26   | 1.86 $\pm$ 0.40     | -10.3 $\pm$ 3.9           | -10.6 $\pm$ 4.9     | 33.6              | 25.4                |
| Dist3 | 6                 | 6                   | 1.14 $\pm$ 0.16   | 1.30 $\pm$ 0.34     | -13.3 $\pm$ 1.1           | -14.9 $\pm$ 1.6     | 41.4              | 37.1                |
| Dist4 | 6                 | 6                   | 1.34 $\pm$ 0.30   | 1.69 $\pm$ 0.44     | -11.8 $\pm$ 0.9           | -12.1 $\pm$ 0.6     | 36.7              | 28.1                |

which indicates there were additional inputs of N from long distance transport (Lee et al., 2016; Zhang et al., 2018). All transects had relatively similar average amounts of summer deposition, with bulk  $\text{N}_{\text{dep}}$  of  $0.84 \pm 0.24 \text{ kg ha}^{-1}$  at the GT transect,  $0.77 \pm 0.17 \text{ kg ha}^{-1}$  at the JH transect, and  $0.79 \pm 0.57 \text{ kg ha}^{-1}$  at the AP transect, but variation within transects was often high. This suggests that transects across the region received similar inputs of N on average, but small-scale topography, vegetation and wind patterns influenced how  $\text{N}_{\text{dep}}$  was distributed across each transect (Kopáček et al., 2012; Weathers et al., 2000, 2006).

Deposition rates measured in this study were higher than those measured in the study area by national monitoring programs. Bulk deposition in our study ranged from 0.26 to  $1.66 \pm 0.35 \text{ kg N ha}^{-1}$  for the summer. There are two National Atmospheric Deposition Program (NADP) sites in the study area: WY08—Yellowstone National Park (YNP) at Tower Falls and WY94-Grand Teton National Park (GTNP). NADP sites measure wet deposition only (National Atmospheric Deposition Program - National Trends Network). In addition, there is a Clean Air Status and Trends Network (CASTNet) (US Environmental Protection Agency Clean Air Markets Division) located in YNP at the

north end of Yellowstone Lake (YEL408). At CASTNet sites, dry deposition of inorganic N species is estimated using measured air concentrations of  $\text{HNO}_3$ ,  $\text{NO}_3^-$  and  $\text{NH}_4$ . Wet deposition in YNP was  $1.21 \text{ kg ha}^{-1}$  ( $0.89 \text{ kg ha}^{-1} \text{ NH}_4\text{-N}$  and  $0.33 \text{ kg ha}^{-1} \text{ NO}_3\text{-N}$ ) in summer 2016 and in GTNP, wet deposition was  $0.20 \text{ kg ha}^{-1}$  ( $0.15 \text{ kg ha}^{-1} \text{ NH}_4\text{-N}$  and  $0.05 \text{ kg ha}^{-1} \text{ NO}_3\text{-N}$ ) for the summer (National Atmospheric Deposition Program - National Trends Network). Dry deposition estimated in YNP in summer 2016 was  $0.02 \text{ kg ha}^{-1} \text{ NH}_4\text{-N}$ ,  $0.004 \text{ kg ha}^{-1} \text{ NO}_3\text{-N}$ , and  $0.05 \text{ kg ha}^{-1} \text{ HNO}_3\text{-N}$  (US Environmental Protection Agency Clean Air Markets Division), for total measured wet and dry deposition of  $1.29 \text{ kg ha}^{-1}$ . This estimate does not include dry  $\text{NH}_3$  and organic N deposition, which modeled values suggest contributed  $1.53 \text{ kg ha}^{-1} \text{ year}^{-1}$  of the total  $1.69 \text{ kg dry N ha}^{-1} \text{ year}^{-1}$  in 2016 (Schwede and Lear, 2014; US Environmental Protection Agency Clean Air Markets Division). A hybrid approach using modeled and measured values in the GYE estimated total dry deposition at  $1.69 \text{ kg N ha}^{-1} \text{ year}^{-1}$  and total wet deposition at  $1.59 \text{ kg N ha}^{-1} \text{ year}^{-1}$  in 2016 (Schwede and Lear, 2014; US Environmental Protection Agency Clean Air Markets Division). This ratio of dry to wet deposition is supported by other

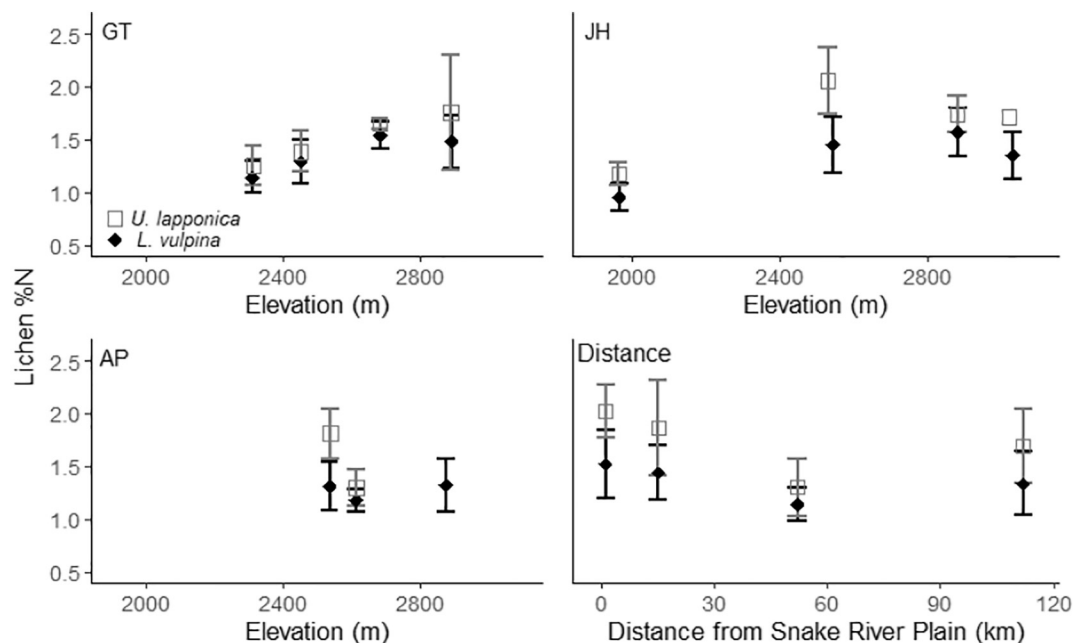


**Fig. 3.** Mean ( $\pm$ 95% CI) nitrogen content (%N) of *U. lapponica* and *L. vulpina* collected from four transects across the Greater Yellowstone Ecosystem near Grand Targhee Ski Resort (GT), Jackson Hole Mountain Resort (JH), Avalanche Peak (AP), and a transect with increasing distance from the Snake River Plain.

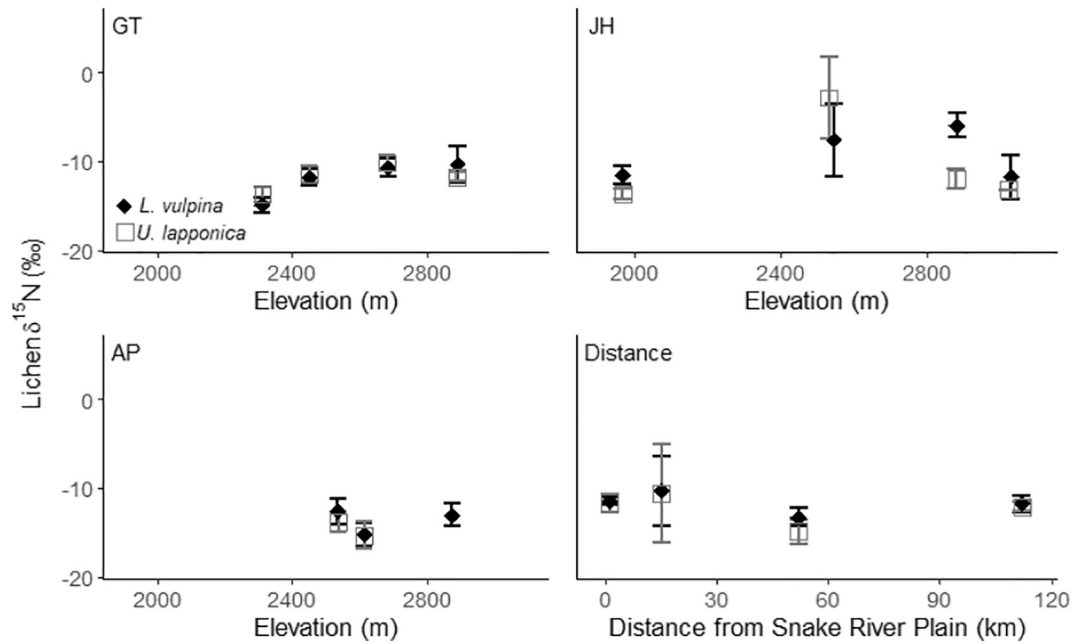


**Fig. 4.** Mean ( $\pm 95\%$  CI)  $\delta^{15}\text{N}$  of *U. lapponica* and *L. vulpina* collected from four transects across the Greater Yellowstone Ecosystem near Grand Targhee Ski Resort (GT), Jackson Hole Mountain Resort (JH), Avalanche Peak (AP), and a transect with increasing distance from the Snake River Plain.

studies in the region that suggest deposition in the area is about 50% wet deposition and 50% dry deposition (Benedict et al., 2013a; Lee et al., 2016). Additionally, 29% and 15% of annual wet deposition was deposited during the summer at NADP sites in YNP and GTNP, respectively (National Atmospheric Deposition Program - National Trends Network). If we assume a conservative estimate of 29% of deposition occurring in the summer, then a rough estimate of annual deposition at our sites would range from  $0.90 \text{ kg N ha}^{-1} \text{ year}^{-1}$  to  $5.72 \text{ kg N ha}^{-1} \text{ year}^{-1}$ . Background deposition rates in the interior mountainous west are estimated around  $1.0 \text{ kg N ha}^{-1} \text{ yr}^{-1}$  or less (Holland et al., 1999; Sverdrup et al., 2012). Approximately  $3 \text{ kg N ha}^{-1} \text{ yr}^{-1}$  is sufficient to alter soils, foliar C:N ratios, water quality and aquatic ecosystems in mountainous environments (Baron et al., 2000; Nanus et al., 2017; Spaulding et al., 2015). The annual rates estimated by our study

would indicate that parts of the GYE, including high elevation areas near Jackson (JH4), the SRP (GT4), and in northeastern Yellowstone National Park (AP3, Dist4) are experiencing negative effects from N deposition.

Our study highlights the amount of variation that can occur over small spatial scales. The AP transect, which spanned the smallest range of elevation and distance, had bulk  $\text{N}_{\text{dep}}$  that spanned the entire range of deposition across all transects. At the GT transect west of the SRP, there was also an increase in bulk  $\text{N}_{\text{dep}}$  and lichen %N at higher elevation sites, where there are also higher rates of precipitation and wet deposition. Similarly,  $\text{N}_{\text{dep}}$  patterns at the JH transect were related to precipitation, as the lowest elevation site had lower  $\text{N}_{\text{dep}}$ , lichen %N, and precipitation, while the three higher elevation sites had comparatively high  $\text{N}_{\text{dep}}$ , lichen %N and precipitation. However, neither of

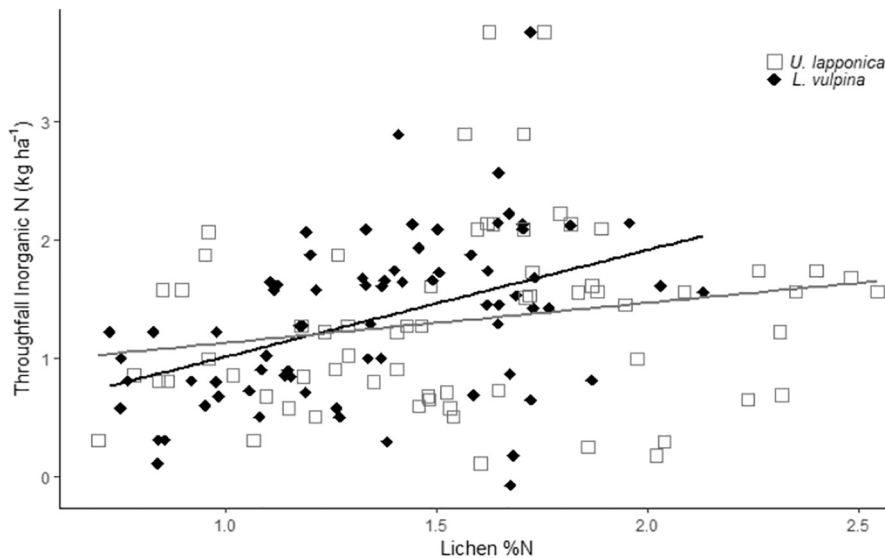


**Fig. 5.** The relationship between %N in two lichen species (*U. lapponica* and *L. vulpina*) and N deposition measured by throughfall collectors located at the tree where each lichen was collected in the Greater Yellowstone Ecosystem. Throughfall deposition was positively correlated with %N in *L. vulpina* ( $p = 0.0001$ ,  $R^2 = 0.19$ ) and the relationship was not significant between throughfall deposition and *U. lapponica* ( $p = 0.11$ ).

these relationships were significant indicating precipitation alone is not driving N patterns in the GYE. Recent studies in the area suggest that dry deposition contributes about 50% of total deposition (Benedict et al., 2013a; Lee et al., 2016; Zhang et al., 2018), so understanding mechanisms that influence dry deposition is necessary to better understand overall deposition patterns. Furthermore, other factors such as slope, edge effects and turbulent atmospheric conditions influence deposition patterns (Kopáček et al., 2012; Weathers et al., 2000, 2006). For example, Prenni et al. (2014) document local thermally driven air circulation on the west side of the Tetons, which explains changes in N concentrations in air masses over the course of a day. The influence of these localized factors on  $N_{dep}$  patterns limits the efficacy of disperse monitoring sites, especially in areas with complex topography such as the GYE.

Although both lichen species showed similar trends in %N, *L. vulpina* typically had lower %N than *U. lapponica* which has been commonly observed in other studies (McMurray et al., 2015, 2013). In the Wind River Range in Wyoming, background deposition rates of  $0.9 \text{ kg N ha}^{-1} \text{ yr}^{-1}$  corresponded with N concentrations below 1.35% in *U. lapponica* and 1.12% in *L. vulpina* (McMurray et al., 2013). At our sites in the GYE, almost all sites had lichen %N above those concentrations which was expected because current N deposition estimated in our study and in modeling studies is  $1\text{--}4 \text{ kg N ha}^{-1} \text{ year}^{-1}$  above background levels (Lee et al., 2016; Zhang et al., 2018). Studies throughout the U.S. Northwest and California found critical levels of  $N_{dep}$  for *L. vulpina* to be  $1.0\text{--}1.02\%$  N, which corresponded to critical loads of  $2.51\text{--}3.1 \text{ kg ha}^{-1} \text{ year}^{-1}$  (Fenn et al., 2008; Root et al., 2015). Similarly, in the Sierra Nevada Range in CA, along a remote road, %N in *L. vulpina* ranged from 0.78 to 1.13%, while %N along a major highway ranged from 1.10 to 2.00% N (Bermejo-Orduna et al., 2014). In our study at 14 out of 15 sites mean *L. vulpina* %N was  $>1.13\%$  N. McMurray et al. (2013) also recorded that lichen %N concentrations at two sites in Wyoming with measured N deposition above  $3.0 \text{ kg N ha}^{-1} \text{ yr}^{-1}$  were 1.90% N in *U. lapponica* and 1.56% N in *L. vulpina*. At our sites we observed similar %N levels near Jackson (JH2, JH3) and the SRP (Dist1).

Lichen C:N ratios generally decrease as  $N_{dep}$  increases, which is indicative of N stress and the inability of mycobiont growth to keep up with photobiont growth spurred by N availability (Palmqvist et al., 2017; Palmqvist and Dahlman, 2006). Additionally,  $N_{dep}$  can lead to acidification of pigments important to photosynthesis, which decreases the lichens ability to obtain C (Carter et al., 2017). Lichens that are known to be tolerant to air pollution can maintain C:N ratios even at high rates of  $N_{dep}$  (Palmqvist and Dahlman, 2006), while shade adapted lichens, with low photosynthesis rates are very sensitive to  $N_{dep}$  (Hauck and Wirth, 2010). The C:N ratios for *L. vulpina* in this study range from 29.4 to 48.7, while for *U. lapponica*, C:N ratios range from 22.7 to 39.2. In comparison, a study on the impacts of traffic on N pollution in the Sierra Nevada in CA, found C:N ratios in *L. vulpina* along a relatively unimpacted forest service road were  $49.2 \pm 5.32$ , while C:N ratios along a major highway were  $33.55 \pm 4.88$  (Bermejo-Orduna et al., 2014). While a clear threshold for C:N ratios that indicate N stress will require more research, C:N ratios in lichens should be further explored as an indicator of how vulnerable an ecosystem is to inputs of N.

Overall, lichen %N was not well correlated with throughfall  $N_{dep}$ . Other studies (McMurray et al., 2013; Root et al., 2013) have reported highly correlated values for IER N and lichen N. However, these studies were conducted in areas with singular point sources that lichens responded to (McMurray et al., 2013), or in areas that have higher precipitation and deposition rates (Root et al., 2013). Additionally, these studies measured annual deposition, had more collectors per site, used the same tree species at each site, and used bulk lichen collections which consists of many lichens, instead of the individual specimen collections in this study. %N in individual lichens is affected by thalli size, metabolic processes, climatic and microhabitat variation across a landscape, such as substrate or differences in relative humidity (Carter et al., 2017; Root et al., 2013). Canopies of different tree species may vary in retention of  $\text{NO}_3^-$  (Fenn et al., 2013) or  $\text{NH}_4$  (Lovett and

Lindberg, 1993). Additionally, canopy density influences dry deposition characteristics of the canopy and the high surface area of conifer canopies may be particularly efficient at scavenging aerosols and cloud deposition, leading to high localized rates of deposition (Weathers et al., 2006). Concentrations of ions and total volumes of throughfall are often higher than stemflow (Pryor and Barthelmie, 2005), so lichen location on a host tree may also influence %N measured in individual lichens. For these reasons, lichen %N may not correlate highly with throughfall  $N_{dep}$  in some environments.

The  $N_{dep}$  measured in throughfall was always higher than the  $N_{dep}$  measured in bulk deposition at the same site, and in some cases, values were 3–4 times higher (Fenn et al., 2003, 2008; Fenn and Poth, 2004). This pattern could reflect several processes, including dry deposition to the vegetation canopy (Hofhansl et al., 2011) leaching of inorganic N from vegetation, or in-canopy processing of N (Cape et al., 2010). However, biological processes often discriminate against heavier isotopes, so if N was leached from canopy tissues or taken up by canopies, the isotope ratios would be different between throughfall and bulk deposition (Heaton et al., 1997).  $\delta^{15}\text{N}\text{-NO}_3^-$  and  $\delta^{15}\text{N}\text{-NH}_4$  were not different between throughfall and bulk collectors, which suggests that the sources of throughfall and bulk deposition are the same and the canopy is concentrating deposition, not leaching ions (Heaton et al., 1997), at least during the summer months. Other studies have also suggested that tree canopies take up  $\text{NO}_3^-$  (Fenn et al., 2013), which could contribute to the low levels of  $\text{NO}_3^-$  deposition observed in this study, but this is not supported by isotope values or differences in  $\text{NH}_4\text{-N}:\text{NO}_3\text{-N}$  ratios in bulk and throughfall deposition in our study. In comparison with the Cape et al. (2010), Heaton et al. (1997), and Fenn et al. (2013) studies, the sites in this study are relatively dry in the summer when collections were made (Table 1), so the absence of N leaching or processing in the canopy could be limited by water availability.

Lichen and deposition isotope values were low across the GYE, which indicates that agriculture is the dominant source of  $N_{dep}$ . Lichen  $\delta^{15}\text{N}$  values mostly range between  $-16\%$  to  $-8\%$ , which are similar to values found in lichens near feedlots and intensive agricultural areas (Boltersdorf and Werner, 2013).  $\delta^{15}\text{N}\text{-NH}_4$  ratios were between  $-5.5\%$  and  $2.7\%$ , except for at four sites discussed below and there was more  $\text{NH}_4$  than  $\text{NO}_3^-$  in deposition at every site. This is consistent with modeling studies that find high deposition contributions from agriculture (Lee et al., 2016; Zhang et al., 2018), field studies that have measured high concentrations of  $\text{NH}_3$  gas on the western side of the Tetons (Benedict et al., 2013a), and NADP deposition measurements that have a majority  $\text{NH}_4\text{-N}$  (National Atmospheric Deposition Program - National Trends Network). However,  $\delta^{15}\text{N}\text{-NH}_4$  ratios measured in the GYE were higher than those in wet deposition in Rocky Mountain National Park (RMNP), which ranged from  $-10\%$  to  $0\%$  (Nanus et al., 2018). Higher  $\delta^{15}\text{N}\text{-NH}_4$  ratios could be indicative of a combustion  $\text{NH}_4$  source (Zhang et al., 2008) or of aerosol formation (Ti et al., 2018). Additionally,  $\delta^{15}\text{N}\text{-NO}_3^-$  values ranged from  $-12.5\%$  to  $-0.7\%$ , except for at two sites discussed below. These values are similar to wet deposition  $\delta^{15}\text{N}\text{-NO}_3^-$  values that ranged from  $-7.6\%$  to  $-1.3\%$  in RMNP (Nanus et al., 2018) and are representative of contributions from vehicular gasoline combustion (Clow et al., 2015; Elliott et al., 2007). Recent N emissions studies show that vehicle emission contributions to  $N_{dep}$  are underestimated (Fenn et al., 2018; Jiang et al., 2018), which could contribute significantly to  $N_{dep}$  in the GYE, particularly during the summertime when millions of visitors travel through the GYE (National Park Service, 2018). This, combined with local topography could be influencing the higher  $\delta^{15}\text{N}$  in lichens at sites in the JH transect, which indicate there are localized sources of  $\text{NO}_x$  from Jackson, WY at least during the summer months. Our study only measured  $\delta^{15}\text{N}$  values in summer deposition and we do not know how lichen  $\delta^{15}\text{N}$  values in deposition fluctuate seasonally, if at all.

The sites with the highest measured  $N_{dep}$  were located on the Yellowstone Plateau, furthest away from regional agricultural sources.



Long range transport of N emitted in Utah and California or beyond may contribute significantly to  $N_{dep}$  in the GYE due to downwelling of air over the Yellowstone Plateau (Lee et al., 2016; Zhang et al., 2018). N transported over long distances in the atmosphere typically deposits on high elevation landscapes, while valleys are more influenced by local sources (Giannoni et al., 2013). This could be reflected in the sharp increase in  $N_{dep}$  measured at the AP transect over a relatively small elevation change. Additionally, the high isotope ratios in deposition at a few sites alluded to above, could be indicative of particulate formation or higher contributions from combustion sources. Two sites had  $\delta^{15}N-NO_3^-$  values of 1.1‰ and 2.0‰ in throughfall deposition and four sites had  $\delta^{15}N-NH_4^+$  values of 6.2‰ in throughfall, and 8.9‰, 13.8‰, and 15.8‰ in bulk deposition. Higher  $\delta^{15}N$  ratios originate from fossil fuel emissions, or from aerosols, because particulate formation favors heavy isotopes, leading to  $\delta^{15}N$  values around 2.0‰ (Ti et al., 2018). This indicates that both agricultural emissions, combustion emissions, and long range transport of emissions contribute significantly to  $N_{dep}$  in the GYE, which is supported by recent modeling studies (Lee et al., 2016; Zhang et al., 2018).

## 5. Conclusions

Overall,  $N_{dep}$  measured in the GYE was high compared to background deposition for a remote, natural area. General elevation and precipitation patterns that drive  $N_{dep}$  were observed at some sites in this study, but variation in  $N_{dep}$  was high due to the complex topography and emissions sources in the region. Deposition sources were primarily agricultural, but high isotope values and high deposition rates in remote areas suggest there is long distance transport of emissions or unaccounted for contributions from vehicle emissions. Lichen %N was related to  $N_{dep}$ , but the correlation was weak, suggesting there may be a lag in lichen response to  $N_{dep}$  or that individual lichen N was influenced by microclimate factors, such as the position in a tree. Bulk collections of many lichen specimens are better correlated to  $N_{dep}$  because the overall collection incorporates variation across many different microhabitats. However, lichen C:N ratios are useful for understanding how an ecosystem is impacted by  $N_{dep}$  and  $\delta^{15}N$  ratios can be used to understand the extent of impact from different sources.  $N_{dep}$  measurements in this study indicate that the GYE is receiving levels of deposition high enough to degrade water and soil quality and begin to impact sensitive plant species. Overall, lichens and IER collectors provide useful estimates of N at small spatial scales that can be used to understand ecosystem impacts and inform land management.

## Acknowledgements

We thank the Greater Yellowstone Coordinating Committee – Clean Air Partnership, UW-NPS Cooperative Research Station, and NASA Wyoming Space Grant for funding this research. We also thank David Mayer, Ryan Reynolds and Will Bowers for assisting with field work. We thank the University of Wyoming Stable Isotope Facility and Geochemistry Laboratory for assistance with chemical analyses. Additionally, this work was supported by the National Science Foundation under Grant No. EPS 1655726. Finally, we thank three anonymous reviewers for their comments that improved this paper.

## References

- Baron, J.S., Rueth, H.M., Wolfe, A.M., Nydick, K.R., Allstott, E.J., Minear, J.T., Moraska, B., 2000. Ecosystem responses to nitrogen deposition in the Colorado Front Range. *Ecosystems* 3, 352–368. <https://doi.org/10.1007/s100210000032>.
- Beem, K.B., Raja, S., Schwandner, F.M., Taylor, C., Lee, T., Sullivan, A.P., Carrico, C.M., McMeeking, G.R., Day, D., Levin, E., Hand, J., Kreidenweis, S.M., Schichtel, B., Malm, W.C., Collett, J.L., 2010. Deposition of reactive nitrogen during the Rocky Mountain airborne nitrogen and sulfur (RoMANS) study. *Environ. Pollut.* 158, 862–872. <https://doi.org/10.1016/j.envpol.2009.09.023>.
- Benedict, K.B., Chen, X., Sullivan, A.P., Li, Y., Day, D., Prenni, A.J., Levin, E.J.T., Kreidenweis, S.M., Malm, W.C., Schichtel, B.A., Collett, J.L., 2013a. Atmospheric concentrations and deposition of reactive nitrogen in Grand Teton National Park. *J. Geophys. Res. Atmos.* 118, 11875–11887. <https://doi.org/10.1002/2013JD020394>.
- Benedict, K.B., Day, D., Schwandner, F.M., Kreidenweis, S.M., Schichtel, B., Malm, W.C., Collett, J.L., 2013b. Observations of atmospheric reactive nitrogen species in Rocky Mountain National Park and across northern Colorado. *Atmos. Environ.* 64, 66–76. <https://doi.org/10.1016/j.atmosenv.2012.08.066>.
- Bernejo-Orduna, R., McBride, J.R., Shiraiishi, K., Elustondo, D., Lasheras, E., Santamaría, J.M., 2014. Biomonitoring of traffic-related nitrogen pollution using *Letharia vulpina* (L.) hue in the Sierra Nevada, California. *Sci. Total Environ.* 490, 205–212. <https://doi.org/10.1016/j.scitotenv.2014.04.119>.
- Bobbink, R., Hicks, K., Galloway, J., Spranger, T., Alkemade, R., Ashmore, M., Bustamante, M., Cinnerby, S., Davidson, E., Dentener, F., Emmett, B., Erisman, J., Fenn, M., Gilliam, F., Nordin, A., Pardo, L., Vries, W. De, 2010. Global assessment of nitrogen deposition effects on terrestrial plant diversity: a synthesis. *Ecol. Appl.* 20, 30–59.
- Boltersdorf, S., Werner, W., 2013. Source attribution of agriculture-related deposition by using total nitrogen and  $\delta^{15}N$  in epiphytic lichen tissue, bark and deposition water samples in Germany. *Isot. Environ. Health Stud.* 49, 197–218. <https://doi.org/10.1080/10256016.2013.748051>.
- Boltersdorf, S.H., Werner, W., 2014. Lichens as a useful mapping tool? An approach to assess atmospheric N loads in Germany by total N content and stable isotope signature. *Environ. Monit. Assess.* 186, 4767–4778. <https://doi.org/10.1007/s10661-014-3736-3>.
- Burns, D.A., 2004. The effects of atmospheric nitrogen deposition in the Rocky Mountains of Colorado and southern Wyoming, USA – a critical review. *Environ. Pollut.* 127, 257–269. [https://doi.org/10.1016/S0269-7491\(03\)00264-1](https://doi.org/10.1016/S0269-7491(03)00264-1).
- Cape, J.N., Sheppard, L.J., Crossley, A., Van Dijk, N., Tang, Y.S., 2010. Experimental field estimation of organic nitrogen formation in tree canopies. *Environ. Pollut.* 158, 2926–2933. <https://doi.org/10.1016/j.envpol.2010.06.002>.
- Carter, T.S., Clark, C.M., Fenn, M.E., Jovan, S., Perakis, S.S., Riddell, J., Schaberg, P.G., Greaver, T.L., Hastings, M.G., 2017. Mechanisms of nitrogen deposition effects on temperate forest lichens and trees. *Ecosphere* 8, 1–26. <https://doi.org/10.1002/ecs2.1717>.
- Clow, D.W., Roop, H.A., Nanus, L., Fenn, M.E., Sexstone, G.A., 2015. Spatial patterns of atmospheric deposition of nitrogen and sulfur using ion-exchange resin collectors in Rocky Mountain National Park, USA. *Atmos. Environ.* 101, 149–157. <https://doi.org/10.1016/j.atmosenv.2014.11.027>.
- Decina, S.M., Templar, P.H., Hutyra, L.R., 2018. Atmospheric inputs of nitrogen, carbon, and phosphorus across an urban area: unaccounted fluxes and canopy influences. *Earth's Future* 6, 134–148. <https://doi.org/10.1002/2017EF000653>.
- Elliott, E.M., Kendall, C., Wankel, S.D., Burns, D.A., Boyer, E.W., Harlin, K., Bain, D.J., Butler, T.J., 2007. Nitrogen isotopes as indicators of NOx source contributions to atmospheric nitrate deposition across the midwestern and northeastern United States. *Environ. Sci. Technol.* 41, 7661–7667. <https://doi.org/10.1021/es070898t>.
- Felix, J.D., Elliott, E.M., 2014. Isotopic composition of passively collected nitrogen dioxide emissions: vehicle, soil and livestock source signatures. *Atmos. Environ.* 92, 359–366. <https://doi.org/10.1016/j.atmosenv.2014.04.005>.
- Felix, D.J., Elliott, E.M., Gish, T., Maghirang, R., Cambal, L., Clougherty, J., 2014. Examining the transport of ammonia emissions across landscapes using nitrogen isotope ratios. *Atmos. Environ.* 95, 563–570. <https://doi.org/10.1016/j.atmosenv.2014.06.061>.
- Felix, J.D., Elliott, E.M., Gay, D.A., 2017. Spatial and temporal patterns of nitrogen isotopic composition of ammonia at U.S. ammonia monitoring network sites. *Atmos. Environ.* 150, 434–442. <https://doi.org/10.1016/j.atmosenv.2016.11.039>.
- Fenn, M.E., Poth, M.A., 2004. Monitoring nitrogen deposition in throughfall using ion exchange resin columns: a field test in the San Bernardino mountains. *J. Environ. Qual.* 33, 2007–2014. <https://doi.org/10.2134/jeq2004.2007>.
- Fenn, M.E., Haeuber, R., Tonnesen, G.S., Baron, J.S., Grossman-Clarke, S., Hope, D., Jaffe, D.A., Copeland, S., Geiser, L., Rueth, H.M., Sickman, J.O., 2003. Nitrogen emissions, deposition, and monitoring in the Western United States. *Bioscience* 53, 391. [https://doi.org/10.1641/0006-3568\(2003\)053\[0391:NEDAMI\]2.0.CO;2](https://doi.org/10.1641/0006-3568(2003)053[0391:NEDAMI]2.0.CO;2).
- Fenn, M.E., Geiser, L., Bachman, R., Blubaugh, T.J., Bytnerowicz, A., 2007. Atmospheric deposition inputs and effects on lichen chemistry and indicator species in the Columbia River Gorge, USA. *Environ. Pollut.* 146, 77–91. <https://doi.org/10.1016/j.envpol.2006.06.024>.
- Fenn, M.E., Jovan, S., Yuan, F., Geiser, L., Meixner, T., Gimeno, B.S., 2008. Empirical and simulated critical loads for nitrogen deposition in California mixed conifer forests. *Environ. Pollut.* 155, 492–511. <https://doi.org/10.1016/j.envpol.2008.03.019>.
- Fenn, M.E., Ross, C.S., Schilling, S.L., Baccus, W.D., Larrabee, M.A., Lofgren, R.A., 2013. Atmospheric deposition of nitrogen and sulfur and preferential canopy consumption of nitrate in forests of the Pacific Northwest, USA. *For. Ecol. Manag.* 302, 240–253. <https://doi.org/10.1016/j.foreco.2013.03.042>.
- Fenn, M.E., Bytnerowicz, A., Schilling, S.L., Vallano, D.M., Zavaleta, E.S., Weiss, S.B., Morozumi, C., Geiser, L.H., Hanks, K., 2018. Science of the total environment on-road emissions of ammonia: an underappreciated source of atmospheric nitrogen deposition. *Sci. Total Environ.* 625, 909–919. <https://doi.org/10.1016/j.scitotenv.2017.12.313>.
- Fremstad, E., Paal, J., Möls, T., 2005. Impacts of Increased Nitrogen Supply on Norwegian Lichen-Rich Alpine Communities: A 10-Year Experiment. vol. 93, pp. 471–481. <https://doi.org/10.1111/j.1365-2745.2005.00995.x>.
- Galloway, J.N., Dentener, F.J., Capone, D.G., Boyer, E.W., Howarth, R.W., Seitzinger, S.P., Asner, G.P., Cleveland, C.C., Green, P.A., Holland, E.A., Karl, D.M., Michaels, A.F., Porter, J.H., Townsend, A.R., Vo, C.J., 2004. Nitrogen cycles: past, present, and future. *Biogeochemistry* 70, 153–226.
- Geiser, L.H., Jovan, S.E., Glavich, D.A., Porter, M.K., 2010. Lichen-based critical loads for atmospheric nitrogen deposition in Western Oregon and Washington Forests, USA. *Environ. Pollut.* 158, 2412–2421. <https://doi.org/10.1016/j.envpol.2010.04.001>.
- Giannoni, S.M., Rollenbeck, R., Fabian, P., Bendix, J., 2013. Complex topography influences atmospheric nitrate deposition in a neotropical mountain rainforest. *Atmos. Environ.* 79, 385–394. <https://doi.org/10.1016/j.atmosenv.2013.06.023>.

- Glavich, D.A., Geiser, L.H., 2008. Potential approaches to developing lichen-based critical loads and levels for nitrogen, sulfur and metal-containing atmospheric pollutants in North America potential approaches to developing lichen-based critical loads and levels for nitrogen, sulfur an. *Am. Bryol. Lichenol. Soc.* 111, 638–649. <https://doi.org/10.1639/0007-2745-111.4.638>.
- Hauck, M., Wirth, V., 2010. Preference of lichens for shady habitats is correlated with intolerance to high nitrogen levels. *Lichenol.* 42, 475–484. <https://doi.org/10.1017/S0024282910000046>.
- Heaton, T.H.E., Spiro, B., Robertson, S.M.C., 1997. Potential canopy influences on the isotopic composition of nitrogen and sulphur in atmospheric deposition. *Oecologia* 109, 600–607.
- Hofer, S., 2003. Determination of Ammonium (Salicylate) in 2M KCl Soil Extracts by Flow Injection Analysis. *QuikChem Method 12-107-06-2-A*. Lachat Instruments, Loveland, CO.
- Hofhansl, F., Wanek, W., Drage, S., Huber, W., Weissenhofer, A., Richter, A., 2011. Topography strongly affects atmospheric deposition and canopy exchange processes in different types of wet lowland rainforest, Southwest Costa Rica. *Biogeochemistry* 106, 371–396. <https://doi.org/10.1007/s10533-010-9517-3>.
- Holland, E.A., Dentener, F.J., Braswell, B.H., Sulzmann, J.M., 1999. Contemporary and pre-industrial global reactive nitrogen budgets author (s): Elisabeth A. Holland, Frank J. Dentener, Bobby H. Braswell and James M. Sulzmann Source: *Biogeochemistry*, Vol. 46, No. 1/3, New Perspectives on Nitrogen Recycling. *Biogeochemistry* 46, 7–43.
- Holmes, R.M., McClelland, J.W., Sigman, D.M., Fry, B., Peterson, B.J., 1998. Measuring  $15\text{N-NH}_4^+$  in marine, estuarine and fresh waters: an adaptation of the ammonia diffusion method for samples with low ammonium concentrations. *Mar. Chem.* 60, 235–243. [https://doi.org/10.1016/S0304-4203\(97\)00099-6](https://doi.org/10.1016/S0304-4203(97)00099-6).
- Jiang, Z., McDonald, B.C., Worden, H., Worden, J.R., Miyazaki, K., Qu, Z., Henze, D.K., Jones, D.B.A., Arellano, A.F., Fischer, E.V., Zhu, L., Boersma, K.F., 2018. Unexpected slowdown of US pollutant emission reduction in the past decade. *Proc. Natl. Acad. Sci.* 115, 201801191. <https://doi.org/10.1073/pnas.1801191115>.
- Johansson, O., Nordin, A., Olofsson, J., Palmqvist, K., 2010. Responses of epiphytic lichens to an experimental whole-tree nitrogen-deposition gradient. *New Phytol.* 188, 1075–1084.
- Kirchner, M., Fegg, W., Rommelt, H., Leuchner, M., Ries, L., Zimmermann, R., Michalke, B., Wallasch, M., Maguhn, J., Faus-Kessler, T., Jakobi, G., 2014. Nitrogen deposition along differently exposed slopes in the Bavarian Alps. *Sci. Total Environ.* 470–471, 895–906. <https://doi.org/10.1016/j.scitotenv.2013.10.036>.
- Knepel, K., 2003. Determination of Nitrate in 2M KCl Soil Extracts by Flow Injection Analysis. *QuikChem Method 12-107-04-1-B*. Lachat Instruments, Loveland CO.
- Kopáček, J., Posch, M., Hejzlar, J., Oulehle, F., Volková, A., 2012. An elevation-based regional model for interpolating sulphur and nitrogen deposition. *Atmos. Environ.* 50, 287–296. <https://doi.org/10.1016/j.atmosenv.2011.12.017>.
- Lee, H.M., Paulot, F., Henze, D.K., Travis, K., Jacob, D.J., Pardo, L.H., Schichtel, B.A., 2016. Sources of nitrogen deposition in Federal Class I areas in the US. *Atmos. Chem. Phys.* 16, 525–540. <https://doi.org/10.5194/acp-16-525-2016>.
- Lieb, A.M., Darrouzet-Nardi, A., Bowman, W.D., 2011. Nitrogen deposition decreases acid buffering capacity of alpine soils in the southern Rocky Mountains. *Geoderma* 164, 220–224. <https://doi.org/10.1016/j.geoderma.2011.06.013>.
- Lloret, J., Valiela, I., 2016. Unprecedented decrease in deposition of nitrogen oxides over North America: the relative effects of emission controls and prevailing air-mass trajectories. *Biogeochemistry* 129, 165–180. <https://doi.org/10.1007/s10533-016-0225-5>.
- Lovett, G.M., Lindberg, S.E., 1993. Atmospheric deposition and canopy interactions of nitrogen in forests. *Can. J. For. Res.* 23, 1603–1616.
- McMurray, J.A., Roberts, D.W., Fenn, M.E., Geiser, L.H., Jovan, S., 2013. Using epiphytic lichens to monitor nitrogen deposition near natural gas drilling operations in the Wind River Range, WY, USA. *Water Air Soil Pollut.* 224, 1487. <https://doi.org/10.1007/s11270-013-1487-3>.
- McMurray, J.A., Roberts, D.W., Geiser, L.H., 2015. Epiphytic lichen indication of nitrogen deposition and climate in the northern rocky mountains, USA. *Ecol. Indic.* 49, 154–161. <https://doi.org/10.1016/j.ecolind.2014.10.015>.
- Munzi, S., Branquinho, C., Cruz, C., Mágua, C., Leith, I.D., Sheppard, L.J., Sutton, M.A., 2019.  $\delta^{15}\text{N}$  of lichens reflects the isotopic signature of ammonia source. *Sci. Total Environ.* 653, 698–704. <https://doi.org/10.1016/j.scitotenv.2018.11.010>.
- Nanus, L., McMurray, J.A., Clow, D.W., Saros, J.E., Blett, T., Gurdak, J.J., 2017. Spatial variation of atmospheric nitrogen deposition and critical loads for aquatic ecosystems in the Greater Yellowstone Area. *Environ. Pollut.* 223, 644–656. <https://doi.org/10.1016/j.envpol.2017.01.077>.
- Nanus, L., Campbell, D.H., Lehmann, C.M.B., Mast, M.A., 2018. Spatial and temporal variation in sources of atmospheric nitrogen deposition in the Rocky Mountains using nitrogen isotopes. *Atmos. Environ.* 176, 110–119.
- National Atmospheric Deposition Program - National Trends Network, d. Seasonal Averages. <http://nadp.slh.wisc.edu/data/sites/list/?net=NTN>, Accessed date: 27 February 2019.
- National Emissions Inventory, 2014. <https://www.epa.gov/air-emissions-inventories/2014> (616).
- National Park Service, 2018. Visitation Statistics. URL. <https://www.nps.gov/yell/planyourvisit/visitationstats.htm>.
- Palmqvist, K., Franklin, O., Näsholm, T., 2017. Symbiosis constraints: strong mycobiont control limits nutrient response in lichens. *Ecol. Evol.* 7, 7420–7433. <https://doi.org/10.1002/ece3.3257>.
- Palmqvist, K., Dahlman, L., 2006. Responses of the green algal foliose lichen *Platismatia glauca* to increased nitrogen supply. *New Phytol.* 171, 343–356. <https://doi.org/10.1111/j.1469-8137.2006.01754.x>.
- Prenni, A.J., Levin, E.J.T., Benedict, K.B., Sullivan, A.P., Schurman, M.I., Gebhart, K.A., Day, D.E., Carrico, C.M., Malm, W.C., Schichtel, B.A., Collett, J.L., Kreidenweis, S.M., 2014. Gas-phase reactive nitrogen near Grand Teton National Park: impacts of transport, anthropogenic emissions, and biomass burning. *Atmos. Environ.* 89, 7490–7756. <https://doi.org/10.1016/j.atmosenv.2014.03.017>.
- Pryor, S.C., Barthelmie, R.J., 2005. Liquid and chemical fluxes in precipitation, throughfall and stemflow: observations from a deciduous forest and a red pine plantation in the midwestern U.S.A. *Water Air Soil Pollut.* 163, 203–227.
- R Core Team, 2018. R: A Language and Environment for Statistical Computing. R Foundation for Statistical Computing, Vienna, Austria.
- Root, H.T., Geiser, L.H., Fenn, M.E., Jovan, S., Hutten, M.A., Ahuja, S., Dillman, K., Schirokauer, D., Berryman, S., McMurray, J.A., 2013. A simple tool for estimating throughfall nitrogen deposition in forests of western North America using lichens. *For. Ecol. Manag.* 306, 1–8. <https://doi.org/10.1016/j.foreco.2013.06.028>.
- Root, H.T., Geiser, L.H., Jovan, S., Neitlich, P., 2015. Epiphytic macrolichen indication of air quality and climate in interior forested mountains of the Pacific northwest, USA. *Ecol. Indic.* 53, 95–105. <https://doi.org/10.1016/j.ecolind.2015.01.029>.
- Schwede, D.B., Lear, G.G., 2014. A novel hybrid approach for estimating total deposition in the United States. *Atmos. Environ.* 92, 207–220. <https://doi.org/10.1016/j.atmosenv.2014.04.008>.
- Sigman, D.M., Casciotti, K.L., Andreani, M., Barford, C., Galanter, M., Böhlke, J.K., 2001. A bacterial method for the nitrogen isotopic analysis of nitrate in seawater and freshwater. *Anal. Chem.* 73, 4145–4153. <https://doi.org/10.1021/ac010088e>.
- Spaulding, S.A., Otu, M.K., Wolfe, A.P., Baron, J.S., 2015. Paleolimnological records of nitrogen deposition in shallow, high-elevation lakes of Grand Teton National Park, Wyoming, U.S.A. *Arct. Antarct. Alp. Res.* 47, 703–717. <https://doi.org/10.1657/AAAR0015-008>.
- Sverdrup, H., McDonnell, T.C., Sullivan, T.J., Nihlgard, B., Belyazid, S., Rihm, B., Porter, E., Bowman, W.D., Geiser, L., 2012. Testing the feasibility of using the ForSAFE-VEG model to map the critical load of nitrogen to protect plant biodiversity in the Rocky Mountain region, USA. *Water Air Soil Pollut.* 223, 371–387.
- Thornton, P.E., Thornton, M., Mayer, B.W., Wilhelm, N., Wei, Y., Devarakonda, R., Cook, R.B., 2014. Daymet: Daily Surface Weather Data on a 1-km Grid for North America, Version 2. [WWW Document]. ORNL DAAC, Oak Ridge, Tennessee, USA.
- Ti, C., Gao, B., Luo, Y., Wang, X., Wang, S., Yan, X., 2018. Isotopic characterization of  $\text{NH}_x\text{-N}$  in deposition and major emission sources. *Biogeochemistry* 138, 85–102. <https://doi.org/10.1007/s10533-018-0432-3>.
- US Environmental Protection Agency Clean Air Markets Division, d. Clean air status trends network. Seasonal total deposition. URL. [www.epa.gov/castnet/](http://www.epa.gov/castnet/), Accessed date: 27 February 2019.
- Vitousek, P.M., Aber, J.D., Howarth, Robert, Likens, W., Matson, G.E., Schindler, P.A., Schlesinger, D.W., William, H., Tilman, D.G., 1997. Human alterations of the global nitrogen cycle: sources and consequences. *Ecol. Appl.* 7, 737–750.
- Weathers, K.C., Lovett, G.M., Likens, G.E., Lathrop, R., 2000. The effect of landscape features on rates of atmospheric deposition. *Ecol. Appl.* 10, 528–540.
- Weathers, K.C., Simkin, S.M., Lovett, G.M., Lindberg, S.E., 2006. Empirical modeling of atmospheric deposition in mountainous landscapes. *Ecol. Appl.* 16, 1590–1607.
- Williams, J.J., Lynch, J.A., Saros, J.E., Labou, S.G., 2017. Critical loads of atmospheric N deposition for phytoplankton nutrient limitation shifts in western U.S. Mountain lakes. *Ecosphere* 8. <https://doi.org/10.1002/ecs2.1955>.
- Zhang, Y., Liu, X.J., Fangmeier, A., Goulding, K.T.W., Zhang, F.S., 2008. Nitrogen inputs and isotopes in precipitation in the North China Plain. *Atmos. Environ.* 42, 1436–1448. <https://doi.org/10.1016/j.atmosenv.2007.11.002>.
- Zhang, R., Thompson, T.M., Barna, M.G., Hand, J.L., McMurray, J.A., Bell, M.D., Malm, W.C., Schichtel, B.A., 2018. Source regions contributing to excess reactive nitrogen deposition in the Greater Yellowstone Area (GYA) of the United States. *Atmos. Chem. Phys.* 18, 12991–13011.